

Derivation of Pharmacophore and CoMFA Models for Leukotriene D₄ Receptor Antagonists of the Quinoliny(bridged)aryl Series

Albert Palomer,* Jaume Pascual, Francesc Cabré, M. Lluïsa García, and David Mauleón

R & D Department, Laboratorios Menarini, S. A., Alfonso XII 587, 08918 Badalona, Spain

Received July 29, 1999

The present work focuses on the study of the three-dimensional (3D) structural requirements for the leukotriene D₄ (LTD₄) antagonistic activity of compounds having the basic quinoliny(bridged)aryl framework. An approach combining pharmacophore mapping, molecule alignment, and CoMFA models was used to derive a hypothesis for a series of LTD₄ antagonists having the basic diaryl-bridged framework. In this compound series, the produced pharmacophore hypotheses have shown to yield molecule alignments suitable to derive valuable CoMFA models. Model selection focused on (1) obtention of coherent modeling results, (2) consistency with the available SAR data, and (3) ability to predict the activity of an independent set of congeneric molecules. This approach resulted in a combined pharmacophore and CoMFA model that can generally represent the antagonistic activity within a log unit of the measured value for compounds of the series. The resulting pharmacophore (model C) consists of an acidic or negative ionizable function (AC), a hydrogen-bond acceptor (HBA), and three hydrophobic regions (HY) and produces chemically meaningful alignments with the most active compounds of the series mapping the pharmacophore in a extended energetically favorable conformation.

Introduction

Naturally occurring peptidoleukotrienes (pLTs)¹ are believed to be involved in the development of immediate airways hyperresponsiveness pathologies, i.e. allergic asthma and rhinitis, etc.² pLT antagonists have demonstrated benefits derived from the blockade at their receptor that may have medical value for the treatment of bronchial asthma and related diseases.^{3–8}

The number and subtypes of pLT receptors in the airways are still a matter of debate with evidence on structurally different receptors in human and guinea pig airways.^{9–11} Indeed, there is hardly any direct evidence that the leukotriene D₄ (LTD₄) receptor–antagonist interaction is unique or that all of the known LTD₄ receptor–antagonist compounds act in a similar preferential fashion.^{10,12} Despite being structurally diverse, most of the known ligands show some common features, i.e. a common overall shape, which may match the leukotriene structure, based on an acidic function connected to a sequence of ring templates. In the absence of any three-dimensional (3D) information on the structure of the receptor, this array of common chemical features encourages the study of the 3D structural requirements at the receptor. This may provide an advantageous starting point for the rational design of new antagonists as well as to understand the existing structure–activity relationships (SAR). On the basis of these limited observations and the knowledge of several structurally diverse LTD₄ receptor antagonist compounds having high affinity for the receptor, some modeling studies have been recently published.^{13–16} Hariprasad and Kulkarni have recently proposed a 3D QSAR model based on the comparison of the biophoric

patterns of structurally different antagonists.¹⁵ In the study, the authors propose alignments in conflict with the generally accepted superimposition of antagonists based on the observed SAR;¹⁶ therefore, although the proposed alignment stimulates a critical evaluation of the generally agreed ideas, we feel that additional experimental is needed in support of the model. Zwaagstra et al. have proposed a common pharmacophoric arrangement based on the superimposition of several structurally different antagonists.¹⁶ In this approach, the highly rigid LTD₄ receptor antagonist VUF-5087 (**1**) was taken as template and the alignments were obtained by rigidly fitting the low-energy conformations of all the compounds onto the template. Although the resulting alignments are of great help in gaining understanding of the bioactive conformation of the most common LTD₄ antagonists and of the receptor–antagonist interactions, the model is biased by the subjective selection of fitting points and of the template conformation. Finally, we described a preliminary alignment model for a collection of LTD₄ antagonists that combined pharmacophore alignments with CoMFA. The model was based on the superposition of structurally diverse compound classes¹⁴ but showed limited predictive ability possibly due to the excess diversity among the set of selected compounds. The main difficulty in the development of reliable alignments is not only the flexibility of most antagonists¹⁶ but also the ambiguity of the receptor–ligand interactions.^{10,12} Therefore, despite the consequent limitations, we preferred to obtain models based on series of congeners which may act in a similar preferential fashion, rather than considering structurally diverse antagonists.

Some compounds having the template quinoliny(bridged)aryl structure are known to tightly bind the pLT receptors, i.e. VUF-5087 (**1**),¹⁶ MK-0476 (**2**),¹⁷ RG-12553 (**3**),¹⁸ and OT-4003 (**4**)¹⁹ (see Figure 1). In addi-

* To whom correspondence should be addressed. Tel: +34-3-4628800/11 (ext 342). Fax: +34-3-4628813. E-mail: apalomer@menarini.es.

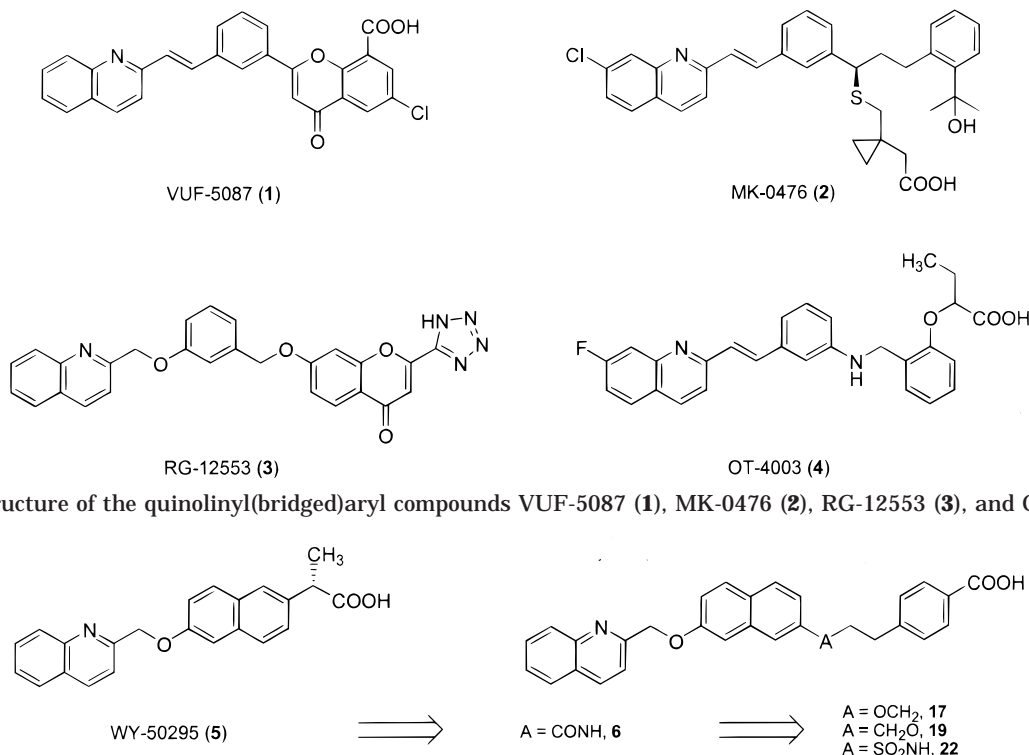


Figure 1. Structure of the quinolinyl(bridged)aryl compounds VUF-5087 (1), MK-0476 (2), RG-12553 (3), and OT-4003 (4).

Figure 2. Structure of the quinolinyl(bridged)aryl compound WY-50295 (5) and 6, 17, 19, and 22, the resulting compounds of the SAR studies on this series.^{14,20,29}

tion, the LTD₄ antagonism program at Laboratorios Menarini led to the evolution of a known 5-lipoxygenase inhibitor of the quinoline compound series, WY-50295 (5), into potent LTD₄ antagonists having the basic quinolinyl(bridged)aryl framework²⁰ (see Figure 2). The activity-improvement process was based on the combined use of classic (structural modification) and computer-aided SAR (pharmacophore and CoMFA models) to establish the geometrical requirements for activity. Since this early modeling study producing pharmacophore and CoMFA models,¹⁴ we observed that the geometry of compounds was a key feature for activity in this series. Therefore, we considered the obtention of improved models for a more accurate prediction of compound activity prior to synthesis. In this article we describe the results of this modeling study leading to improved pharmacophore and CoMFA models accounting for the activity of a congeneric series of LTD₄ antagonists having the basic quinolinyl(bridged)aryl framework. Our approach focused not only on the yield of coherent modeling results, i.e. correlation parameters and model significance, but also on consistency with the SAR data and the usefulness and predictivity of the resulting tools.

Although a number of applications of CoMFA to medicinal chemistry have been reported,^{21–23} it is well-accepted that flexible molecules are by far the most difficult when analyzing ligands to generate a CoMFA model.²³ When there are no structural data available, one of the most critical steps in CoMFA methodology is the selection of the conformation for each ligand in the series, followed by molecular superimposition (alignment rules). Moreover, it is well-accepted that in the process of binding a ligand to a protein, there is not necessarily a unique solution and, therefore, multiple binding modes are possible.²⁴ Several methodologies

have been developed to try to solve these problems:^{25–28} e.g. pharmacophore maps have been used as the set of rules for molecule alignment prior to CoMFA. Although this methodology offers a suitable “alignment model”, the fundamental problem is that the proposed solution is often not unique; i.e. it offers multiple solutions to the alignment problem. The present study deals with a set of flexible molecules and no structural knowledge of the receptor site. We tried to overcome the difficulties on conformer selection and alignment of flexible molecule by using a pharmacophoric “alignment rule” and considering one alignment per molecule, or taking two closely related ones in the limited cases where the conformation selection is ambiguous. In such cases, the alignments were chosen among the energetically accessible conformers considering the molecule fit into the pharmacophore and a common overlay onto the most active compound of the series, 1. Then selection was done on the basis of improving the Q^2 obtained with CoMFA. This step was realized in an attempt to improve the reliability of the final results, yet despite the risk of data overfit in the Q^2 -based selection process, we expect clear advantages based on the use of such models. At this time, when a single conformer of a given molecule is chosen in the final model, this approach allows selection of the most suitable conformation which may relate to the “bioactive” one. In contrast, when several different conformers are included, they may account for slightly diverse positions of binding. The procedure does not intend to differentiate among different binding modes but rather to improve the subjective conformer selection process previous to CoMFA choosing among slightly different alignments for which objective selection is ambiguous. Moreover, the inclusion of extreme diverse geometrical dispositions and alignments may generate a completely different CoMFA

Table 1. Predicted vs Actual pK_i Values for the Learn and Test Sets of Compounds Obtained Using the Combined Alignment C and CoMFA Model III

learn set	K_i actual (nM) ^a	pK_i actual	pK_i calcd (fitting) ^b	test set	K_i actual (nM) ^a	pK_i actual	pK_i calcd (predict) ^c
6	1.05 ± 0.08	9.0	8.6/8.8 ^d	9	3.4 ± 1.9	8.5	8.0
7	1.5 ± 0.25	8.8	8.7	11	15 ± 1	7.8	8.4
8	7.8 ± 2	8.1	8.2	14^g	9.0 ± 3	8.0	7.4
10^f	13 ± 2	7.9	7.9	16	4.0 ± 0.6	8.4	8.2
12	30 ± 5	7.5	7.7	17	5.6 ± 0.4	8.3	8.4
13	30 ± 6	7.5	7.2	18	21 ± 8	7.7	7.5
15	15 ± 2	7.8	8.2	20	7.3 ± 2	8.1	8.2
19	2.7 ± 0.4	8.6	8.7	21	4.6 ± 2.7	8.3	7.8
22	2.6 ± 0.1	8.6	8.7	23	13 ± 2	7.9	7.8
24	4.1 ± 0.4	8.4	8.6	26	2.4 ± 1.2	8.6	7.8
25	3.8 ± 0.3	8.4	8.5	27	8.4 ± 3	8.1	7.3
28	70 ± 12	7.2	7.3	29	9.2 ± 2	8.0	7.4
31	12 ± 3	7.9	inactive ^h	30	5.5 ± 0.5	8.3	7.5
32	68 ± 5	7.2	<i>e</i>	33	29 ± 3	7.5	8.0
34	134 ± 18	6.9	6.8	37	34 ± 5	7.5	8.0
35	118 ± 1	6.9	6.8	39	190 ± 21	6.7	6.7
36	36 ± 13	7.4	7.4	40	360 ± 63	6.4	7.2
38	38 ± 6	7.4	7.7	43	7.3 ± 3.6	8.1	7.1
41	30 ± 1	7.5	7.4	44	88 ± 7	7.1	7.8
42	28 ± 3	7.6	7.1	45	297 ± 79	6.6	6.5
47	250 ± 90	6.6	7.0	46	4.8 ± 0.01	8.3	7.7
48	86 ± 21	7.1	inactive ^h	49	108 ± 43	7.0	7.4
52	168 ± 58	6.8	6.6	50	44 ± 15	7.4	8.1
55	inactive	6.0	<i>e</i>	51	595 ± 119	6.2	6.7
56	79 ± 18	7.1	7.7	53	40 ± 4	7.4	6.9
57	1054 ± 220	6.0	<i>e</i>	54	2590 ± 848	5.6	6.3
58	inactive	6.0	6.2	60^g	inactive	6.0	8.5
59^g	237 ± 50	6.6	<i>e</i>				

^a Activity in the in vitro ³H-LTD₄ binding assay evaluated using guinea pig lung membranes to generate inhibition constants K_i [a value of $K_i = 2.1 \pm 0.5$ nM was obtained for the standard compound MK-0476 (2)]. The data are means ± SD of at least three determinations.

^b Obtention of the CoMFA model III: internal prediction of pK_i values for the learn set of compounds. ^c Validation of the final CoMFA model III: prediction of the pK_i values for the test set of compounds. ^d For **6** no single alignment could be unambiguously chosen; therefore, an additional conformer alignment was selected. ^e Compounds **32**, **55**, **57**, and **59** were omitted in model III. ^f Activity was determined on the acid analogue of the tetrazole compound **10**. ^g Activity was determined on the tetrazole analogue of the carboxylates **14**, **59**, and **60**. ^h Compounds **31** and **48** did not properly map the pharmacophore and therefore were predicted to have low activity.

environment (grids, calculations, etc.) rendering misleading and inconsistent results.

Results and Discussion

Our goal was to derive a putative geometry for the pharmacophore, which should integrate the activity across the collection of molecules having the basic diaryl-bridged framework. The structural series of molecules used in this study is shown in Table 1 and Figure 3 and has been described in the literature.^{14,20,29} The activity was described in an in vitro ³H-LTD₄ binding assay evaluated using guinea pig lung membranes to generate inhibition constants K_i (converted into the $-\log K_i$ (pK_i) for purposes of this modeling study).

The collection of 28 structurally congeneric antagonists shown in Table 1 and Figure 3 was modeled and used as "learn set" to derive the pharmacophore and CoMFA models. Further, a congeneric series of 27 compounds (see Table 1 and Figure 3) was used as genuine "test set" to select the most suitable alignment model. The combined approach is summarized as follows: (1) Obtention of pharmacophore models based on the "learn set" of 28 compounds and the hypothesis generation tools implemented in Catalyst.^{30,31} (2) Alignment of the "learn set" of compounds using the pharmacophore hypotheses and the fitting option implemented in the program. (3) Obtention of the corresponding 3D QSAR model based on the above alignments and derived from CoMFA.²¹ (4) Alignment of the "test set"

of 27 compounds using the pharmacophore hypotheses and the fitting option implemented in the program. (5) Based on the corresponding CoMFA models, prediction of the activity of the aligned molecules of the independent "test set".

Among the proposed hypotheses, the final pharmacophore model was selected on the basis of the following criteria: (1) The most active compounds should be geometrically able to map all pharmacophore elements; meanwhile inactive compounds, which appear to possess the pharmacophore elements, should not be capable of attaining the 3D pharmacophore geometry. (2) The correlation parameters obtained with the optimized CoMFA. (3) Comparison of the capabilities to predict the activity of the compounds of the independent "test set". As a result of this work, we propose improved pharmacophore and CoMFA models accounting for the LTD₄ receptor antagonistic activity of compounds having the basic quinolinyl(bridged)aryl framework. The results emerged as a valuable tool not only to validate the proposed alignment model but also to illustrate and guide some of the steps in the activity-improvement process. A more complete description of the results and their use follows.

Generation of Pharmacophore Models and Molecule Alignments. The pharmacophore hypotheses were obtained from the "learn set" of 28 congeneric molecules (see Table 1 and Figure 3). Among the generated hypotheses, A–C were selected on the basis of a proper activity estimation (correlation coefficient

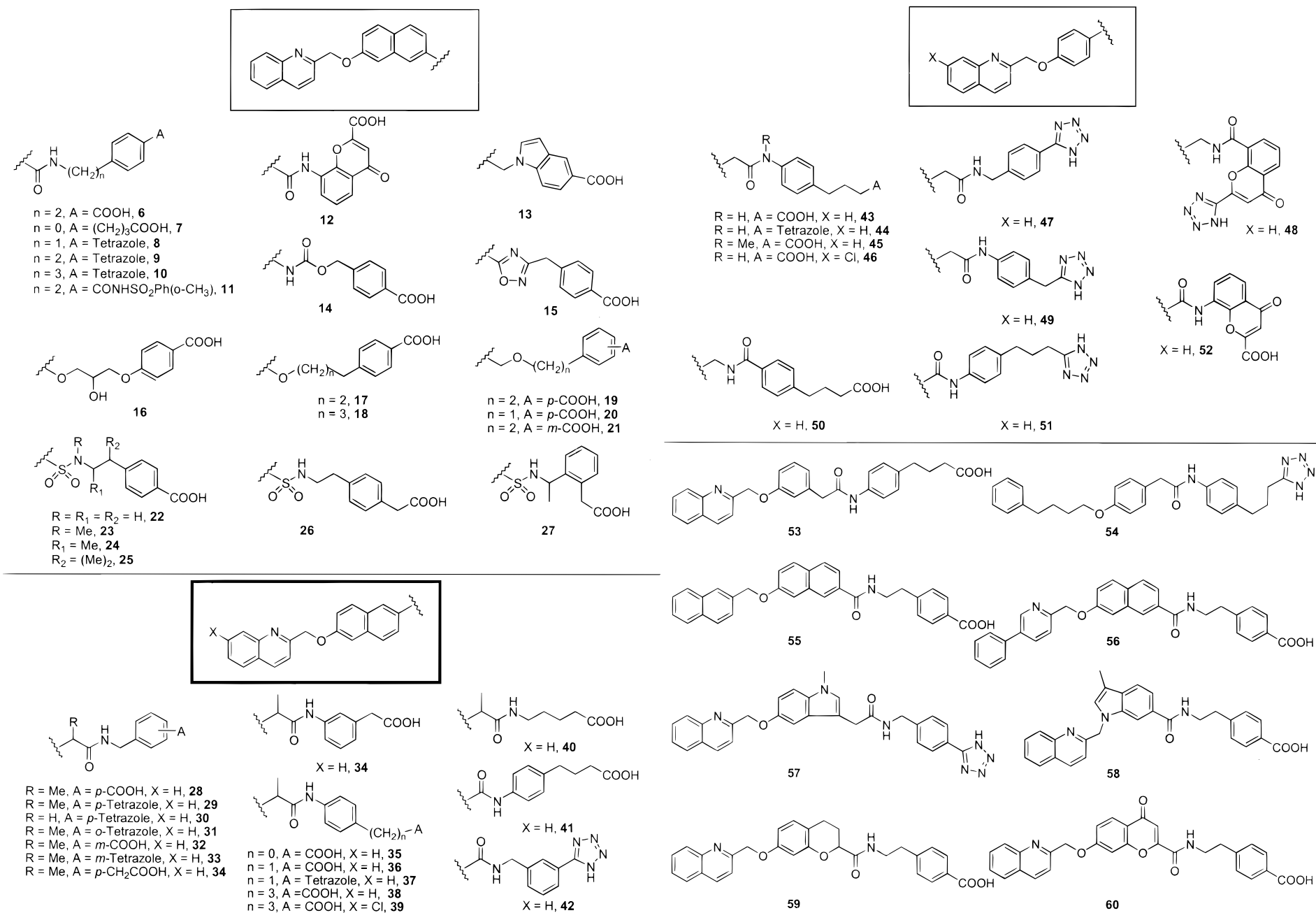


Figure 3. Chemical structure of the diaryl-bridged compounds used to derive the pharmacophore and CoMFA models.^{14,20,29}

Table 2. Correlation Coefficient (Predicted vs Actual Activity) for the Selected Hypotheses A–C^a

hypothesis	correlation coefficient	hypothesis features ^b
A	0.8642	3 HY groups, 1 HBA, and 1 (neg) AC group
B	0.8509	3 HY groups, 1 HBA, and 1 (neg) AC group
C	0.9022	3 HY groups, 1 HBA, and 1 (neg) AC group

^a The regression lines that correlate for each hypothesis the actual vs estimated activity values, as implemented within Catalyst, were used to select the models A–C. ^b The library of chemical features within the program was used to map the chemical functionalities in each molecule.

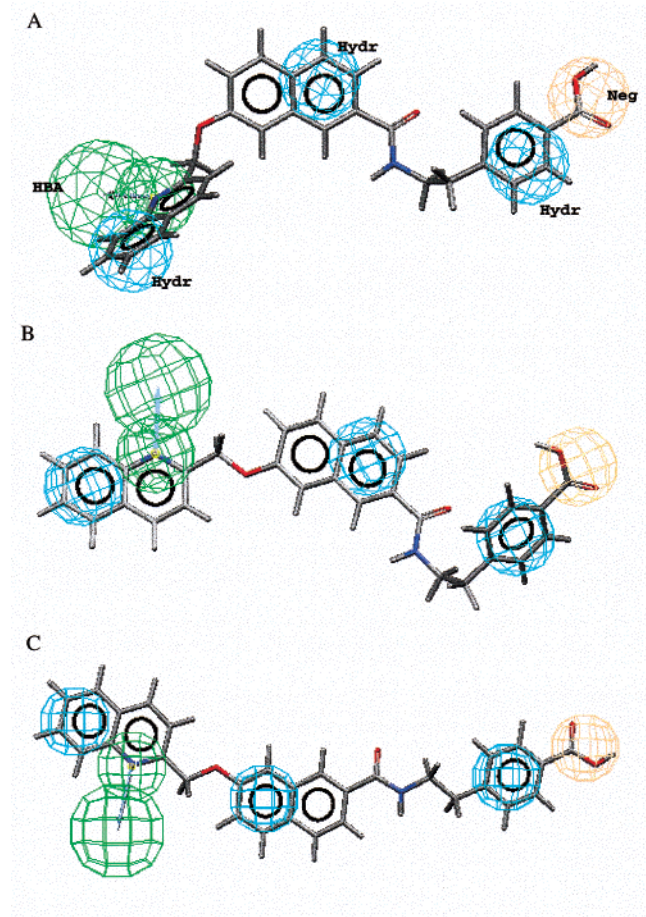


Figure 4. Pharmacophore models A–C with **6** fitted. The three pharmacophores consist of an acidic or negative ionizable chemical function (Neg), a hydrogen-bond acceptor (HBA), and three hydrophobic regions (Hydr). The chemical features are drawn as globes. Only HBA is shown by two globes due to the directional nature of this chemical function.³²

of the predicted vs actual activities) and criteria of optimum pharmacophore mapping and overall superposition of the most active compounds onto **6** (see Table 2 and Materials and Methods for details). All three hypotheses consist of five chemical features in different geometric dispositions: an acidic or negative ionizable function (AC), three hydrophobic regions (HY), and, importantly, a hydrogen-bond acceptor (HBA). The models are shown in Figure 4 with compound **6** fitted. The chemical features are drawn as globes. Only HBA is shown by two globes due to the directional nature of this chemical function.³² Importantly, the HBA feature present in all three models is consistent with the results obtained by Masamune et al.³³ The authors described that the nitrogen atom present in the quinoline or

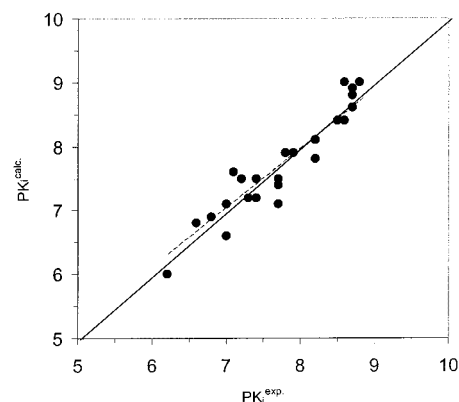


Figure 5. Observed vs predicted pK_i values for the “learn set” of compounds (fitting) obtained with the alignment C and model III. Dashed line indicates the linear regression.

substituted pyridine side chain of a class of agents exemplified by VUF-5087 (**1**; see Figure 1) is essential for potent activity.

On the basis of the generated conformational models and the pharmacophore hypothesis, several alignments, which do not alter the geometry of the conformers, may be obtained per molecule using a rigid fit approach (FAST fitting tools within Catalyst). In the present study we selected one alignment per molecule taking into consideration criteria of low-conformational energy and optimum overall superposition onto **6**. Exceptionally, single-conformer selection was not unique for compounds **6**, **41**, and **56** and a two-conformation model had to be used. In contrast, compound **52** was not able to map pharmacophore A and **31** and **48** could not map hypothesis C; therefore, the compounds were predicted to have low activity and were omitted from the corresponding compound collection.

Obtention of CoMFA Models. The molecule alignments on the pharmacophore suggested by Catalyst were used as input for CoMFA. Hence, the CoMFA models I–III were based on the molecule alignments on the pharmacophore hypotheses A–C, respectively. Summaries of the resulting correlations are shown in Table 3 and Figure 5.

The corresponding CoMFA models were derived, and selection of compounds/conformers was based on Q^2 improvement criteria (see Materials and Methods for details). In the present study, the process for compound selection forced to delete **42**, **47**, and **55–59** from the initial collection in model I, **13**, **31**, **47**, **55**, and **57** in model II, and **32**, **55**, **57**, and **59** in model III. Although the inactive compounds **57** ($pK_i = 6.0$) and **59** ($pK_i = 6.6$) share most structural features with the other components of the set, these compounds are representative of a unique structural modifications in the central aromatic ring region. Indeed, these molecules present in this region indoles or a 2,3-dihydro-4*H*-1-benzopyran ring (see Figure 3). Similarly, **55** (inactive) and **56** ($pK_i = 7.1$), having a 2-naphthyl or 2-phenylpyridyl group instead of the basic 2-quinolinyl, represent the only variations of this latter. Hence, it is not surprising that these compounds, representatives of unique structural modifications, had to be omitted in order to obtain acceptable Q^2 values. Consequently, the models are expected to hardly predict compounds with severe structural modification in the quinolinyl moiety and the

Table 3. CoMFA–PLS Analysis of LTD₄ Antagonists Based on the Alignments A–C Suggested by Catalyst^a

CoMFA model	alignment	no. of compd	CoMFA field ^c	learn set ^b				test set ^h	
				Q^2_{LOO} (<i>N</i>)	PRESS	P^2	<i>S</i>	no. of compd	<i>R</i>
I	A	20 ^{d,e}	ste + ele	0.56 (4)	0.50	0.997	0.04	30	0.25
II	B	23 ^f	ste + ele	0.50 (4)	0.63	0.975	0.14	30	0.21
III	C	22 ^{d,g}	ste + ele	0.74 (3)	0.38	0.960	0.15	30	0.70
III (ele)	C	22	ele	0.74 (5)	0.47				
III (ste)	C	22	ste	0.73 (4)	0.49				

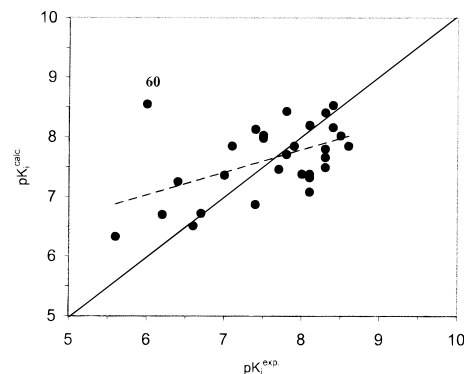
^a The leave-one-out cross-validated r^2 (Q^2_{LOO}) and explanatory r^2 (P^2) values were obtained with regard to the optimum number of components listed in the table (*N*). ^b "Learning set" of compounds (see Table 1 and Figure 3). ^c Steric (ste), electrostatic (ele), or both CoMFA fields were used as input for the PLS analysis. ^d Compound **52** in model I as well as compounds **31** and **48** in model III did not properly map the pharmacophore and, therefore, were predicted to be inactive and were omitted from the PLS analysis. ^e Compounds **42**, **47**, and **55–59** were omitted in model I. ^f Compounds **13**, **31**, **47**, **55**, and **57** were omitted in model II. ^g Compounds **32**, **55**, **57**, and **59** were omitted in model III. ^h "Test set" for models I–III consisted of an independent collection of compounds (see Table 1 and Figure 3).

central aromatic region. Finally, compounds **13** ($pK_i = 7.5$), **31** ($pK_i = 7.9$), **32** ($pK_i = 7.2$), **42** ($pK_i = 7.5$), and **47** ($pK_i = 6.6$) appear to possess the proper pharmacophore elements able to attain the 3D pharmacophore geometry; therefore, elimination is probably due to an inadequate selection of the conformer alignment.

Activity Prediction and Pharmacophore Selection. The obtention of sufficient statistical results in a CoMFA model based on a given molecule alignment adds in support of the selected alignment rules but it is not conclusive on the real meaning of the alignment nor on the consistency of the collection of molecules considered. Therefore, although the statistical results obtained for the CoMFA model shed some light on the most coherent set of molecule alignments, we preferred to use independent criteria to evaluate the proposed hypotheses A–C. The combined pharmacophore–CoMFA predictive tool was used to predict the activity of an independent set of 27 congeneric compounds (the "test set"; see Table 1 and Figure 3). The compounds were modeled; then conformer/alignments were selected for each pharmacophoric hypothesis (A–C), and the activity was predicted with the CoMFA models I–III, respectively. The results are summarized in Table 3.

On the basis of both the statistical parameters obtained and the predictive ability of the resulting models, pharmacophore C and CoMFA model III were selected. The final model presented the following correlation parameters: $Q^2 = 0.74$, $S_{\text{PRESS}} = 0.38$ (3 optimum components), conventional $P^2 = 0.960$, and standard error of estimate = 0.15. In addition, correlation was analyzed separately with the steric and electrostatic components of CoMFA. Similar statistical results were obtained for each field separately (steric $Q^2 = 0.73$ and electrostatic $Q^2 = 0.74$). Despite the major contribution of steric field in final CoMFA models, the equivalent correlation obtained (results not shown) for each of the fields suggests similar relevance.

In general, satisfactory predictions were obtained with this model except for the outlier molecule **60**. Estimation of the test set activities (including outlier **60**) produced a correlation coefficient of the predicted vs actual activities of 0.70 (*R*; see Table 3). Compound **60** shares most structural features with the other components of the set but represents a unique structural modification in the central aromatic ring region, i.e. a chromone ring (see Figure 3). As explained above, the compound selection used to obtain the CoMFA model forced to delete from the learn set the compounds having modifications in the central aromatic region (**57** and **59**);

**Figure 6.** Observed vs predicted pK_i values for the "test set" of compounds (prediction) obtained with the alignment C and model III. Dashed line indicates the linear regression.

hence, it is not surprising that **60** is hardly predicted by the model. Similarly, **55** presents a particular modification in the quinolinyl region, and this compound was deleted from the learn set; consequently, the models are expected to hardly predict compounds with severe structural modification in the quinolinyl region. Finally, compounds **31**, **32**, and **48** were omitted from the model since no acceptable alignments on the pharmacophore could be found. This fact illustrates the critical aspects of alignment selection in the combined pharmacophore–CoMFA methodology since, although all appear to possess the proper elements able to attain the pharmacophore features, the geometric disposition is inconsistent with the selected model.

The QSAR produced by CoMFA is usually represented as a 3D "coefficient contour" map (see Figures 7 and 8). In the electrostatic map, two intense regions seem to be relevant. The first region, where negative electrostatic interactions are desirable, is consistently near the negatively charged function present in the majority of compounds, i.e. carboxylic acid or tetrazole. In addition, a large region, where positive electrostatic interactions are desirable, encircles the zone where the amide group of **6** is placed. In the steric maps, an "allowed" region surrounded by two "forbidden" regions arranged in a sandwich form forms the region of space accommodating the benzoate in **6**. This suggests the extreme importance of the nature, size, and geometry of this aromatic ring. The region of space accommodating the quinolinyl ring is surrounded by an "allowed" region suggesting that bulkier substitutions or enlarged cycles may be active. The latter may account for a hydrophobic volume that consistently accommodates the 4-phenyl-2-pyridyl ring of compound **56** ($pK_i = 7.1$). On the other hand, the

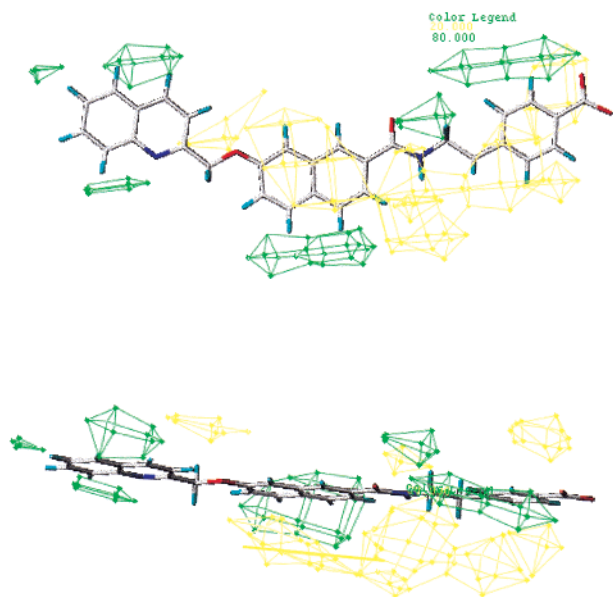


Figure 7. Graphical representation of the steric contour maps for the CoMFA STDEV*COEFF (images are rotated 90° around the *y* axis). Compound **6** is shown as reference. Regions colored yellow (20% contribution) and green (80% contribution) correspond to sterically favorable and unfavorable zones, respectively.

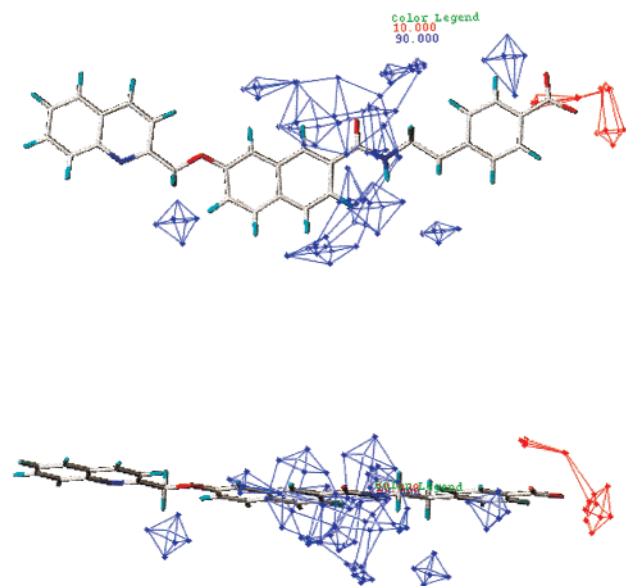


Figure 8. Graphical representation of the electrostatic contour maps for the CoMFA STDEV*COEFF (images are rotated 90° around the *y* axis). Compound **6** is shown as reference. Regions colored red (10% contribution) and blue (90% contribution) correspond to favorable and unfavorable zones, respectively.

steric map consists of two more zones where steric contributions are favorable for activity suggesting favorable substitution positions: one is placed near the characteristic central aryl group (facing the 4,5-substitution positions in the naphthyl of **6**) and another is near the ethylene linker in **6** successfully explored in **24** ($pK_i = 8.4$) and **25** ($pK_i = 8.4$). In contrast, a large nonallowed steric region limits the central part of the molecules suggesting the importance of the overall geometry, consistently with the experimental observations that suggest a favorable 2,7- rather than 2,6-substitution

pattern in the central naphthalene ring: i.e. **9** (1.5 nM) vs **29** (9.2 nM) or **30** (5.5 nM), **6** (1.05 nM) vs **28** (70 nM), and **8** (7.8 nM) vs **35** (118 nM).

The ultimate evidence for the validity of the combined pharmacophore–CoMFA models is the predictive ability. In fact, the potential strength is that they could prioritize synthetic targets or identify and computationally screen novel scaffolds. It is clear from Table 1 and the discussion above that the combined approach can generally represent the activity within a log unit of the measured value for compounds having the basic quinolinyl(bridged)aryl framework. Moreover, results obtained are coherent with the SAR data available, and within this structural series, the models are able to classify compounds based on the overall geometry of the molecules. Finally, the model produces chemically meaningful alignments with the most active compounds of the series mapping the pharmacophore in an extended energetically favorable conformation (see Figure 4).

Conclusions

Some compounds having the template quinolinyl-(bridged)aryl structure are known to tightly bind the pLT receptors (see Figures 1 and 2). In the absence of any 3D information on the structure of the receptor, it is important to obtain models accounting for the 3D structural requirements at the receptor. These models may be useful to prioritize synthetic targets or to identify and computationally screen novel scaffolds. The present work focuses on the use of existing methods to develop such predictive models and to understand the 3D structural requirements at the LTD₄ receptor. An approach combining pharmacophore mapping, molecule alignment, and CoMFA models was used to derive a hypothesis for a series of LTD₄ antagonists having the basic diaryl-bridged framework. The selection of the pharmacophore and CoMFA models focused on the ability to estimate the activity of an independent set of congeneric compounds and also on the obtention of coherent modeling results and consistency with the SAR data. The produced pharmacophore model C consists of five chemical features (see Figure 4): an acidic or negative ionizable function (AC), a hydrogen-bond acceptor (HBA), and three hydrophobic regions (HY). The produced pharmacophore has shown to yield molecule alignments suitable to derive valuable CoMFA models indicative of a good predictive tool. As a result, we propose improved pharmacophore and CoMFA models accounting for the LTD₄ receptor antagonistic activity of compounds having the basic diaryl-bridged structural framework. Importantly, the most active compounds map the pharmacophore in an extended energetically accessible conformation; i.e. the selected alignments are chemically meaningful, and the current models generate one of the possible active conformations for this series of compounds.

Materials and Methods

The structural series of compounds having the basic diaryl framework used in this study has been previously described in the literature^{14,20,29} with their activity in an in vitro ³H-LTD₄ binding assay evaluated using guinea pig lung membranes to generate inhibition constants K_i . The K_i values have been converted into the $-\log K_i$ (pK_i) for purposes of this molecular modeling study.

Molecular Modeling. All molecular modeling studies were performed on a Silicon Graphics Personal Iris 4D35 computer running Catalyst software version 2.2 (Molecular Simulations Inc., San Diego, CA) and Sybyl software version 6.1 (Tripos Associates, St. Louis, MO). The basic modeling methodologies leading to the pharmacophore-based alignments (e.g. conformational analysis, molecule fitting, etc.) were performed within Catalyst using the implemented chemical features^{30,32} and the energy minimization procedure using a standard conjugate gradients minimization algorithm and a modified version of CHARMM molecular mechanics force field.³⁴ The underlying operation of the Catalyst software has already been described in detail.³⁰ Conformational analysis was performed as implemented in the program using the above-described minimizer coupled to a "poling" function to assess conformational variation³⁵ and the BEST algorithm which intends to optimize the conformational coverage versus the size of the assembly.^{36,37} In the calculation, a threshold of 250 conformers per molecule and a maximum of 20 kcal/mol were used. Fitting of a molecule onto the pharmacophore was performed within Catalyst taking into account the chemical features present in the molecule. The library of chemical descriptors within the program³² was used to map the chemical functionalities in each molecule; then fitting operations were done using the FAST algorithm which does not alter the geometry of the molecule (rigid fit). On the other hand, the basic CoMFA methodology was applied following the general approach described by Cramer et al.²¹ CoMFA fields (steric and electrostatic) were calculated using the Tripos force field with a C_{sp}3 probe with a charge of +1. Atomic charges were obtained on the ionized form of the molecules using MOPAC 6.0 (AM1). A standard CoMFA lattice was used with a 2 Å grid spacing. Correlations were derived with the PLS method with cross-validation on the leave-one-out mode except for the final model where no cross-validation was used. In the final model, the number of components was determined using *S*_{PRESS} as the criterion. The PLS analyses were performed, respectively, with scaling of the steric and electrostatic contributions according to the standard CoMFA deviations as implemented in the program. In general, it was our intention to follow the "Recommendations for CoMFA Studies and 3D QSAR Publications" published by Thibaut et al.³⁸

Pharmacophore Hypothesis Generation. The process followed for pharmacophore hypothesis generation was based on the methodology implemented in Catalyst and consists of the following steps: (1) conformational search as described above using the implemented force field and a poling function to ensure conformational diversity; (2) mapping the chemical functionalities of each molecule and conformer; (3) identification of common chemical features and valid geometric arrangement of the chemical functions to generate pharmacophoric hypotheses;³² (4) for each hypothesis, geometric fit of the molecules by superimposing equivalent functional groups without modifying the geometry of the molecule (rigid fit operation); and (5) analysis of the generated hypotheses. Each hypothesis carries two regression lines that correlate the activity of each molecule with the geometric fit onto the pharmacophore (activity estimation tool) and the estimated vs actual activity values (correlation tool), the latter being useful to test the validity of each model. In the present work, the pharmacophore hypotheses were obtained from the "learn set" collection of 28 congeneric molecules having the basic diaryl-bridged framework (see Table 1 and Figure 3). The models A–C were selected among the generated hypotheses using the above-described activity correlation tool implemented in Catalyst (see Table 2 for the results on models A–C) together with visual criteria of optimum pharmacophore mapping and overall superposition of the most active compounds onto lead compound 1.

Obtention of CoMFA Models. CoMFA models were built with the "learn set" collection of 28 congeneric molecules and using the molecule alignments onto the selected pharmacophore hypotheses A–C proposed by Catalyst. Taking into account the collection of conformers considered, several alignments

may be obtained per molecule using the rigid fit operations implemented in the program. From this collection, one conformer alignment was selected per molecule taking into consideration criteria of low conformational energy, optimum pharmacophore mapping, and overall superimposition onto 6. Exceptionally, single-conformer selection was not unique for compounds 6, 41, and 56 and a two-conformation model had to be used. Further, the selected alignments onto each of the hypotheses A–C were used to develop the corresponding CoMFA models I–III, respectively, following the general CoMFA approach described above. In order to improve the reliability of the final model (*Q*² values), some compounds were selected for deletion from the initial collection. The default implementation of PLS statistical tools and graphics within Sybyl was used for compound selection with special focus on the activity prediction plot (predicted vs actual activities) and the *Q**Q* plot (distribution of residuals compared to that expected for a normal Gaussian distribution). The final CoMFA models I–III present the correlation parameters shown in Table 3.

Activity Prediction and Pharmacophore Model Selection. The molecule alignment on each of the pharmacophore hypotheses A–C and the corresponding CoMFA models I–III further served for activity prediction of the collection of 27 congeneric compounds described in Table 1 ("test set"). The results are summarized in Table 3. First, several alignments on the pharmacophore model were obtained per molecule taking into account the collection of conformers considered and using the rigid fit operations implemented in the program. Among this collection, one conformer alignment per molecule was selected taking into consideration criteria of low conformational energy, optimum pharmacophore mapping, and overall superposition onto 6. For compounds 6, 52, and 57 no single alignment could be unambiguously chosen, and therefore an additional alignment was selected. Further, antagonist p*K*_i values were predicted for each aligned molecule using the CoMFA model and following the general CoMFA methodology described above. On the basis of the model correlation parameters and the prediction results of pharmacophores A–C (CoMFA models I–III, respectively; see Table 3), the pharmacophore alignment C was selected.

Acknowledgment. The authors thank Dr. A. Giolitti (Menarini Ricerche S.p.A.) for helpful discussions and assistance in reviewing the manuscript.

References

- (1) Borgeat, P.; Samuelsson, B. Metabolism of Arachidonic Acid in Polymorphonuclear Leukocytes: Structural Analysis of Novel Hydroxylated Compounds. *J. Biol. Chem.* **1979**, *254*, 7865–1869.
- (2) Hammarstrom, S.; Murphy, R.; Samuelsson, B.; Clark, D. A.; Mioskowski, C. Ch.; Corey, E. J. Structure of Leukotriene C. Identification of the Amino acid Part. *Biochem. Biophys. Res. Commun.* **1979**, *91*, 1266–1268.
- (3) Borgeat, P.; Samuelsson, B. Arachidonic Acid Metabolism in Polymorphonuclear Leukocytes: Effects of Ionophore A23187. *Proc. Natl. Acad. Sci. U.S.A.* **1979**, *76*, 2148–2152.
- (4) Borgeat, P.; Samuelsson, B. Transformation of Arachidonic Acid by Rabbit Polymorphonuclear Leukocytes: Formation of Novel Dihydroxyeicosatetraenoic Acid. *J. Biol. Chem.* **1979**, *254*, 2643–2646.
- (5) Fort-Hutchinson, A. W. Leukotriene Antagonists and Inhibitors: Clinical Applications. *Adv. Prostaglandin, Thromboxane, Leukotriene Res.* **1995**, *23*, 69–74.
- (6) Larsen, J. S.; Acosta, E. P. Leukotriene-Receptor Antagonists and 5-Lipoxygenase Inhibitors in Asthma. *Ann. Pharmacother.* **1993**, *27*, 898–903.
- (7) Chung, K. F. Leukotriene Receptor Antagonists and Biosynthesis Inhibitors: Potential Breakthrough in Asthma Therapy. *Eur. Respir. J.* **1995**, *8*, 1203–1213.
- (8) Pauwels, R. A.; Joos, G. F.; Kips, J. C. Leukotrienes as Therapeutic Target in Asthma. *Allergy* **1995**, *50*, 615–622.
- (9) Taylor, I. K. Cysteinyl Leukotrienes in Asthma: Current State of Therapeutic Evaluation. *Thorax* **1995**, *50*, 1005–1010.
- (10) Smith, L. J. Leukotrienes in Asthma: the Potentials Therapeutic Role of Antileukotriene Agents. *Arch. Intern. Med.* **1996**, *156*, 2181–2189.
- (11) Barnes, N. Leukotriene Receptor Antagonists: Clinical Effects. *J. R. Soc. Med.* **1997**, *90*, 200–204.

- (9) Nicosia, S.; Capra, V.; Giovanazzi, S.; Rovati, E. Binding Sites for Peptido-Leukotrienes in Human Lung Parenchyma. In *Int. Acad. Biomed. Drug Res.*; Langer, S. Z., Church, M. K., Nicosia, S., Eds.; Karger: Basel, 1993; Vol. 6, pp 86–90.
- (10) Nicosia, S.; Capra, V.; Ragnini, D.; Giovanazzi, S.; Mezzeti, M.; Kepler, D.; Müller, M.; Rovati, G. E. Receptors for Cysteinyl Leukotrienes in Human Lung Parenchyma: Characterization by Computer Modelling and Photoaffinity Labeling of Binding Sites. In *Advances in Prostaglandin, Thromboxane and Leukotriene Research*; Samuelsson, B., Ed.; Raven Press Ltd.: New York, 1995; pp 267–269. Capra, V.; Rovati, G. E.; Bianchi, M.; Mezzeti, M.; Nicosia, S. Computer Analysis of a Possible Model for Cysteinyl Leukotrienes Receptors in Human Lung Membranes. *Br. J. Pharmacol.* **1994**, *111* (Suppl.), Abstr. 324p.
- (11) Nicosia, S. Pharmacological Characteristics of Leukotriene Antagonists. *Monaldi Arch. Chest. Dis.* **1996**, *51*, 556–564.
- (12) Zhang, M.-Q.; Zwaagstra, M. E.; Nederkoorn, P. H. J.; Timmerman, H. The Role of Arginine in the Binding of LTD₄ Antagonists to CysLT₁ Receptors of Guinea Pig Lung. *Bioorg. Med. Chem. Lett.* **1997**, *7*, 1331–1336.
- (13) Terada, H.; Goto, S.; Hori, H.; Taira, Z. In *QSAR and Drug Design – New Developments and Applications*; Fujita, T., Ed.; 1995; pp 341–367. Hermann, R. B.; Herron, D. K. OVID and SUPER: Two Overlap Programs for Drug Design. *J. Comput.-Aided Mol. Des.* **1991**, *5*, 511–524.
- (14) Palomer, A.; Giolitti, A.; García, M. L.; Cabré, F.; Mauleón, D.; Carganico, G. Molecular Modeling and CoMFA Investigations on LTD₄ Receptor Antagonists. In *QSAR and Molecular Modelling: Concepts, Computational Tools and Biological Applications*; Sanz, F., Manaut, F., Eds.; Prous Science: Barcelona, 1995; pp 444–450. Palomer, A.; Cabré, F.; García, M. L.; Mauleón, D.; Gaillard, P.; Carrupt, P. A.; Testa, B. 3D QSAR Studies on LTD₄ Receptor Antagonism. XIth European Symposium on Structure–Activity Relationships: Computer-Assisted Lead Finding and Optimization, Lausanne, 1996; P70D.
- (15) Hariprasad, V.; Kulkarni, V. M. A Proposed Common Spatial Pharmacophore and the Corresponding Active Conformations of Some Peptide Leukotriene Receptor Antagonists. *J. Comput.-Aided Mol. Des.* **1996**, *10*, 284–292.
- (16) Zwaagstra, M. E.; Timmerman, H.; van de Stolpe, A. C.; de Kanter, F. J. J.; Tamura, M.; Wada, Y.; Zhang, M. Q. Synthesis and Structure–Activity Relationships of Carboxyflavones as Structurally Rigid CysLT₁ (LTD₄) Receptor Antagonists. *J. Med. Chem.* **1998**, *41*, 1428–1438. Zwaagstra, M. E.; Schoenmakers, S. H. H. F.; Nederkoorn, P. H. J.; Gelens, E.; Timmerman, H.; Zhang, M. Q. Development of a Three-Dimensional CysLT₁ (LTD₄) Antagonist Model with an Incorporated Amino Acid Residue from the Receptor. *J. Med. Chem.* **1998**, *41*, 1439–1445.
- (17) Labelle, M.; Belley, M.; Gareau, Y.; Gauthier, J. Y.; Guay, D.; Gordon, R.; Grossman, S. G.; Jones, T. R.; Leblanc, Y.; McAuliffe, M.; McFarlane, C.; Masson, P.; Metters, K. M.; Ouimet, N.; Patrick, D. H.; Piechuta, H.; Rochette, C.; Sawyer, N.; Xiang, Y. B.; Pickett, C. B.; Ford-Hutchinson, A. W.; Zamboni, R. J.; Young, R. N. Prostaglandin E₂ Receptor. *Bioorg. Med. Chem. Lett.* **1995**, *5*, 283–289.
- (18) Huang, F. C.; Galembo, R. A.; Poli, G. B.; Learn, K. S.; Morissette, M. M.; Johnson, W. H.; Dankulich, W. P.; Campbell, H. F.; Carnathan, G. W.; VanInwegen, R. G. Development of a Novel Series of (2-Quinolinylmethoxy)phenyl Containing Compounds as High-affinity Leukotriene D₄ Receptor Antagonists 4) Addition of Chromone Moiety Enhances Leukotriene D₄ Receptor Binding Affinity. *J. Med. Chem.* **1991**, *34*, 1704–1709.
- (19) Kirstein, D.; Neilson, C. K.; Bramm, E. OT-4003 a Potent Long-acting Orally Active Leukotriene D₄ Receptor Antagonist. *Inflamm. Res.* **1995**, *44* (Suppl. 3), S261 (Abstr. W11/20).
- (20) Pascual, J.; Fos, E.; García, M. L.; Borràs, L.; Montserrat, X.; Palomer, A.; Cabré, F.; Carabaza, A.; García, A. M.; Fernández, M. F.; Calvo, L.; Ferrer, X.; Mauleón, D.; Carganico, G. A New Series of Quinoline Derivatives as LTD₄ Antagonists. XIIIth International Symposium in Medicinal Chemistry, Paris, 1994; P184. Pascual, J.; García, M. L.; Borràs, L.; Montserrat, X.; González, G.; Santiso, S.; Fernández, M.; Andreu, J. A.; Palomer, A.; Cabré, F.; Carabaza, A.; García, A. M.; Ferrer, X.; Calvo, L.; Tost, D.; Ortega, E.; Mauleón, D. A New Series of Quinoliny Methoxy Naphthyl Derivatives as LTD₄ Antagonists. XIVth International Symposium in Medicinal Chemistry, Maastricht, 1996; P230.
- (21) Cramer III, R. D.; Patterson, D. E.; Bunce, J. D. Comparative Molecular Field Analysis (CoMFA) Effect of Shapes on Binding of Steroids to Proteins. *J. Am. Chem. Soc.* **1988**, *110*, 5959–5967.
- (22) Martin, Y. C.; Lin, C. T.; Wy, L. Application of CoMFA to D1 Dopaminergic Agonists: A Case Study. In *3D QSAR in Drug Design*; Kubinyi, H., Ed.; ESCOM: Leiden, 1993; pp 643–660.
- (23) Klebe, G.; Abraham, U. On the Prediction of Binding Properties of Drug Molecules by Comparative Molecular Field Analysis. *J. Med. Chem.* **1993**, *36*, 70–80.
- (24) Mattos, C.; Ringe, D. Multiple Binding Modes. In *3D QSAR in Drug Design*; Kubinyi, H., Ed.; ESCOM: Leiden, 1993; pp 226–254.
- (25) Marshall, G. R.; Barry, C. D.; Bosshard, H. E.; Dammkoehler, R. A.; Dunn, D. A. A Conformational Parameter in Drug Design: The Active Analogue Approach. *ACS Symp. Series* **1979**, *112*, 205–226.
- (26) Martin, Y. C.; Bures, M. G.; Danaher, E. A.; DeLazzer, J. New Strategies that Improve the Efficiency of the 3D Design of Bioactive Molecules. In *Trends in QSAR and Molecular Modeling 92*; Wermuth, C., Ed.; ESCOM: Leiden, 1993; pp 20–26.
- (27) Oprea, T. I.; Waller, C. L.; Marshall, G. R. Three-dimensional Quantitative Structure Activity Relationship of Human HIV (I) Protease Inhibitors. 2. Predictive Power Using Limited Exploration of Alternate Binding Sites. *J. Med. Chem.* **1994**, *37*, 2206–2012.
- (28) Nicklaus, M. C.; Milne, G. W. A.; Burke, T. R. QSAR of Conformationally Flexible Molecules: CoMFA of Protein-Tyrosine Kinase Inhibitors. *J. Comput.-Aided Mol. Des.* **1992**, *6*, 487–504.
- (29) Cabré, F.; Carabaza, A.; García, A. M.; Calvo, L.; Ferrer, X.; Ruiz, A.; Cama, C.; Sánchez, J.; Ucedo, P.; Evangelista, S.; Tramontana, M.; Palomer, A.; García, M. L.; Mauleón, D.; Carganico, G. Pharmacology of LM-1376, a Novel, Potent and Selective Leukotriene D₄ Receptor Antagonist. *Inflamm. Res.* **1995**, *44*, S260. Cabré, F.; Carabaza, A.; García, A. M.; Calvo, L.; Rotllán, E.; Ferrer, X.; Cama, C.; Sánchez, J.; Vázquez, M. C.; Ucedo, P.; Pascual, J.; Palomer, A.; García, M. L.; Mauleón, D. Pharmacology of New Orally Active Leukotriene D₄ Receptor Antagonists: LM-1426, LM-1453 and LM-1468. *Prostagl. Leukotr., Essent. Fatty Acids* **1996**, *55*, 104.
- (30) Sprague, P. W. Automated Chemical Hypothesis Generation and Database Searching with Catalyst. In *Perspectives in Drug Discovery and Design*; Müller, K., Ed.; ESCOM, Leiden, 1995; pp 1–20. Kaminski, J. J.; Rane, D. F.; Snow, M. E.; Weber, L.; Rothofsky, M. L.; Anderson, S. D.; Lin, S. L. Identification of Novel Farnesyl Protein Transferase Inhibitors Using Three-Dimensional Database Searching Methods. *J. Med. Chem.* **1997**, *40*, 4103–4112. Keller, P.; Bowman, M.; Dang, K. H.; Garner, J.; Leach, S. P.; Smith, R.; McCluskey, A. Pharmacophore Development for Corticotropin-Releasing Hormone: New Insights into Inhibitor Activity. *J. Med. Chem.* **1999**, *42*, 2351–2357.
- (31) Catalyst version 2.2, Molecular Simulations Inc., San Diego, CA.
- (32) Greene, J.; Kahn, S.; Savoj, H.; Sprague, P.; Teig, S. Chemical Function Queries for 3D Database Search. *J. Chem. Inf. Comput. Sci.* **1994**, *34*, 1297–1308.
- (33) Masamune, H.; Eggler, J. F.; Marfat, A.; Melvin, L. S.; Rusek, F. W.; Tickner, J. E.; Cheng, J. B.; Shirley, J. T. LTD₄ receptor binding activity of novel pyridine chromanols: Qualitative correlation with pK(a). *Bioorg. Med. Chem. Lett.* **1995**, *5* (13), 1371–1376.
- (34) Brooks, B. R.; Bruccoleri, R. E.; Olafson, B. D.; States, D. J.; Swaminathan, S.; Karplus, M. CHARMm: A Program for Macromolecular Energy, Minimization and Dynamics Calculations. *J. Comput. Chem.* **1983**, *4*, 187–196.
- (35) Smellie, A. S.; Teig, S. L.; Towbin, P. Poling: Promoting Conformational Variation. *J. Comput. Chem.* **1995**, *16*, 171–176.
- (36) Smellie, A. S.; Kahn, S. D.; Teig, S. L. Analysis of Conformational Coverage. 1. Validation and Estimation of Coverage. *J. Chem. Inf. Comput. Sci.* **1995**, *35*, 285–292.
- (37) Smellie, A. S.; Kahn, S. D.; Teig, S. L. Analysis of Conformational Coverage. 2. Application of Conformational Models. *J. Chem. Inf. Comput. Sci.* **1995**, *35*, 295–301.
- (38) Thibaut, U.; Folkers, G.; Klebe, G.; Kubinyi, H.; Merz, A.; Rognan, D. Recommendations for CoMFA Studies and 3D QSAR Publications. In *3D QSAR in Drug Design*; Kubinyi, H., Ed.; ESCOM: Leiden, 1993; pp 711–716. Thibaut, U.; Folkers, G.; Klebe, G.; Kubinyi, H.; Merz, A.; Rognan, D. Recommendations for CoMFA Studies and 3D QSAR Publications. *Quant. Struct.-Act. Relat.* **1994**, *13*, 1–3.

JM990387K